

Leveraging Quantum Superposition to Infer the Dynamic Behavior of a Spatial-Temporal Neural Network Signaling Model

Gabriel A. Silva

Department of Bioengineering and Department of Neurosciences
 Center for Engineered Natural Intelligence and Kavli Institute for Brain and Mind
 University of California San Diego, La Jolla CA 92093 USA

Email: gsilva@ucsd.edu

Abstract. The exploration of new problem classes for quantum computation is an active area of research. In this paper, we introduce and solve a novel problem class related to dynamics on large-scale networks relevant to neurobiology and machine learning. Specifically, we ask if a network can sustain inherent dynamic activity beyond some arbitrary observation time or if the activity ceases through quiescence or saturation via an 'epileptic'-like state. We show that this class of problems can be formulated and structured to take advantage of quantum superposition and solved efficiently using the Deutsch–Jozsa and Grover quantum algorithms. To do so, we extend their functionality to address the unique requirements of how input (sub)sets into the algorithms must be mathematically structured while simultaneously constructing the inputs so that measurement outputs can be interpreted as meaningful properties of the network dynamics. This, in turn, allows us to answer the question we pose.

Contents

1	Introduction	2
2	Overview of the Problem Set Up and Solution	3
2.1	Problem Set Up	3
2.2	Overview of the Solution	4
3	Refractory and Signal Latency Dynamics in Geometric Neural Networks	5
3.1	The Refraction Ratio and its Effects on Dynamics	6
3.2	Prior Work	6
3.3	Mathematical Introduction to the Model	8
3.3.1	Geometric network construction	8
3.3.2	Refractory period and signal dynamics	9
3.3.3	Internal dynamics of v_j	9
3.3.4	Refraction ratio and signal competition	10
3.3.5	Bounds and constraints on Δ_{ij}	10
3.3.6	Effective refractory period and temporal offsets	10

3.3.7	Extended refraction ratio	11
3.4	Analysis of Activation Conditions	11
3.4.1	Theorems for determining activation vertices	12
3.5	Extensions Beyond the Basic Construction	12
3.5.1	Probabilistic extension	12
3.5.2	Inhibitory inputs into v_j	13
3.5.3	Fractional summation of contributing signaling events	13
4	Preparing Network States for Deutsch-Jozsa Computations	15
4.1	Set Membership Conditions	15
4.2	Functional Interpretations of $F(V, T_o)$ Outcomes	16
4.3	Determining Membership in S_n and S_n^c Using Grover's Algorithm	17
4.3.1	Construction of the oracle function	17
4.3.2	Diffusion operator and search space	18
4.3.3	Iterative application of Grover's algorithm	18
4.3.4	Probabilistic nature and verification	18
5	Evaluating Network Dynamics with the Deutsch-Jozsa Algorithm	18
5.1	Evaluating S_n and S_n^c with a Two-Part U_f	19
5.1.1	Behavior for S_n	19
5.1.2	Behavior for S_n^c	19
5.2	Constructing U_f to Evaluate $f(S_n)$	19
5.2.1	Example of a Binary Subtraction for Evaluating $f(S_n)$	20
5.3	Measurement Interpretations of U_f	21
6	Comparative Algorithmic Complexity	21
6.1	Classical complexity	21
6.2	Quantum complexity: Grover's algorithm	21
6.3	Quantum complexity: Deutsch–Jozsa Algorithm	22
6.4	Comparative analysis	22
7	Discussion	23
7.1	Modeling the Evolution of Network Dynamics Beyond T_o	24
7.2	Open Questions and Future Directions	25

1 Introduction

Research into quantum computing applications has historically focused on a few well-established topics. These include cryptography, data security, and the simulation of complex physical and chemical systems, including quantum mechanics itself [1, 2, 3, 4, 5, 6].

However, exploring new problem classes that are particularly suitable for quantum computation is an active area of research. This includes both the application of existing quantum algorithms and the development of new ones. For example, Google Quantum and X Prize recently announced a competition to promote the development of practical, real-world quantum computing algorithms and applications (<https://www.xprize.org/prizes/qc-apps>).

One of the unique challenges of exploring the applicability of quantum computing is that there is no known or obvious process for systematically structuring problems or questions to conform to the mathemat-

ical and algorithmic requirements of quantum computation. The structure and solution of each problem are essentially a bespoke pursuit. A well-posed problem needs to leverage quantum properties such as superposition, entanglement, and interference so that measurement outcomes are meaningful and interpretable to the question being addressed. Achieving this requires designing problems that can demonstrate the computational advantages of quantum algorithms while also showing their relevance to practical or theoretical topics and problems of interest.

In this paper, we introduce and solve a novel problem class related to dynamics on large-scale networks relevant to neurobiology and machine learning. Specifically, given a particular spatial (geometric)-temporal neural signaling model, we ask if a network can sustain inherent dynamic activity beyond some arbitrary observation time or if the activity ceases through quiescence or saturation via an 'epileptic'-like state. In a neuroscientific context, this question informs how and when brain networks can encode and represent information given their physical structural and temporal properties. In the context of machine learning, this work relates to understanding activation patterns in artificial neural networks, which have implications for stability, efficiency, and memory.

From a computational perspective, solving this problem classically requires brute-force evaluation of the network's state by assessing the internal state of each node individually, an approach that is increasingly computationally expensive and eventually prohibitive for very large networks. **We show that this problem can be formulated and structured to take advantage of quantum superposition and solved efficiently using the Deutsch–Jozsa and Grover quantum algorithms.** To do so, we extend their functionality to address the unique requirements of how input (sub)sets into the algorithms must be mathematically structured while simultaneously constructing the inputs so that measurement outputs can be interpreted as meaningful properties of the network dynamics. This, in turn, allows us to answer the question we pose.

Our intent here is twofold. First, it demonstrates a proof-of-concept application of quantum computing to a network dynamics problem with theoretical significance in neuroscience and machine learning. Second, it provides a systematic framework for thinking about and structuring problems in a way that exploits the advantages of quantum computing, contributing to the broader effort of exploring quantum computing's applicability to new types of problems and questions.

The logical flow of the paper is as follows: We first introduce the network dynamic model. We then formally define the problem that we aim to answer. We then describe how the quantum algorithms can be adapted and extended to solve the problem efficiently. **Specifically, the main intellectual contributions are in the ability to take a sophisticated neurodynamical model and re-frame it in a set-theoretic way that conforms to the structural input requirements of the Deutsch-Jozsa algorithm, such that simultaneously, the measurement outputs are interpretable behaviors of the network dynamics.** We then provide formal proofs of complexity advantages and numerical demonstrations of speedups for the quantum versus purely classical approach to solving the problem.

2 Overview of the Problem Set Up and Solution

2.1 Problem Set Up

We aim to address a specifically constructed question regarding the dynamics of neural networks by leveraging the uniquely quantum property of superposition. The specific problem we address is the following: **After some period of dynamic evolution, can the dynamics (i.e., activity) of a neural network sustain inherent activity beyond an arbitrary observation time T_o , or are the dynamics guaranteed to stop, either due to 'epileptic'-like saturation or quiescence?**

By *inherent dynamic activity*, we mean the ability of the neurons (nodes) within the network to continue firing and maintaining the network's internal dynamics autonomously without requiring an external driving input. The network functions as a self-sustaining system where activity persists due to its internal structure and the interactions between connected nodes.

By *epileptic*, we mean a state where all neurons in the network fire simultaneously at the observation time T_o . If this occurs, the dynamics will likely perpetuate indefinitely, maintaining a state of uniform and saturated firing beyond T_o . More precisely, the probability of this outcome depends on the network's connectivity, geometry, firing frequencies, and the internal dynamic state of the neurons. We assume here that when all neurons fire simultaneously, the dynamics are likely to enter this saturated state, a condition we have previously shown theoretically and in numerical experiments [7, 8].

In contrast, *quiescence* refers to the complete cessation of neuronal firing across the network, resulting in no continued activity without external input or stimulation. Again, this is a condition we have reported on in prior published work [7]; see also Figure 1. below.

Much of the technical setup will be in defining and describing the neural dynamic model we will be using. While this is not the only model we could have explored, we chose it because:

1. It is derived from foundational physical and neurophysiological principles (spatial and temporal summation) relevant to neurobiological neurons.
2. It is computationally tractable and builds directly on prior work.
3. It is of relevance to real neurobiological systems. We have previously shown how individual neurons and networks of neurons (connectomes) use the model's specific theoretical and computational properties as a functional optimization principle.
4. Its computational outputs exhibit sufficient complexity to make the application of quantum superposition both challenging and insightful.

2.2 Overview of the Solution

After introducing the model and describing it mathematically, we then show how to map the network dynamics question into a framework suitable for quantum computation. This involves formulating the problem to exploit quantum superposition using the Deutsch-Jozsa and Grover algorithms. We will show that the quantum computations result in interpretable output measurements that enable us to infer whether the network dynamics can sustain inherent activity or cease through epileptic-like saturation or quiescence. By carefully structuring the problem, we will show that a quantum algorithmic solution is computationally more efficient than purely classical methods.

The Deutsch-Jozsa algorithm is a quantum computing algorithm designed to efficiently determine whether a function behaves the same way for all its inputs, outputting either all 0's or all 1's (constant), or if the output is an equal mix of 0's and 1's (balanced). In our case, we provide the algorithm a list of 0's and 1's that encode the activation (firing) patterns representing the network's dynamics. The algorithm processes this information all at once, leveraging the quantum property of superposition. If the outputs are *all* 0's or *all* 1's (constant), we interpret the network's activity pattern as being either in a quiescent state (if all 0's), where no activity happens, or in an epileptic-like state (if all 1's), where everything fires at once. If the outputs are not all the same, it implies the network's dynamics are more complex, with activity in the network having the potential to continue processing information.

However, there's a challenge: the Deutsch-Jozsa algorithm requires evaluating all possible patterns of

activity in the network at once, including patterns that did not actually occur in the network. This would make the algorithm’s output impossible to interpret in terms of the network’s real dynamics. To work around this, we divide the problem into two parts. First, we focus only on the patterns of activity that actually occurred in the network. For the patterns that did not occur, we assign them fixed, known values (either 0 or 1), depending on how we are running the algorithm.

This approach allows us to run the Deutsch-Jozsa algorithm twice in the following way. In the first run, we assign all non-occurring patterns a value of 0. In the second run, we assign them a value of 1. The patterns of activity that actually occurred are already encoded in the collection of observed or measured values of 0’s and 1’s. If the output of the algorithm in the first run (where non-occurring patterns were assigned 0’s) is all 0’s, this implies that the activity patterns in the network were also all 0’s, meaning the network was in a quiescent state. Similarly, if the output of the second run (where non-occurring patterns were assigned 1’s) is all 1’s, it implies that the network was in an epileptic-like state. If the outputs are not constant (i.e., not all 0’s or not all 1’s) in either case, it implies that the activity patterns in the network were a mix of 0’s and 1’s, and we interpret this as the network having the potential to sustain dynamic activity.

By interpreting the outputs of these two runs, we can derive the state of the activity pattern of the network and determine if the activity can continue or if it stops. *The quantum computational advantage lies in the fact that we do not need to evaluate each pattern individually, one at a time. Instead, the Deutsch-Jozsa algorithm evaluates the entire set of patterns simultaneously in superposition, saving an enormous amount of computational effort.* The larger the network being interrogated, the greater the computational speedup and resource savings achieved through this approach.

3 Refractory and Signal Latency Dynamics in Geometric Neural Networks

The network dynamic model we will use operates on structural geometric networks. It is effectively a sophisticated geometric extension of the classical integrate-and-fire model. This model takes into account the neurobiologically canonical processes of spatial and temporal summation of discrete signaling events (action potentials) incident on nodes (neurons) within a geometric network. We define a *geometric network* as a physically constructible structural network where the edges between neurons are convoluted paths with physical distances. In a neurobiological context, this corresponds to the path lengths of axons and dendrites that connect chemical synapses between neurons, making the model anatomically accurate. The inclusion of network geometry and finite signaling speeds (conduction velocities) of action potentials naturally introduces signaling latencies.

The dynamic and diverse arrival and summation of action potentials at individual neurons, combined with a neuronal refractory period (described below), determine when neurons fire. It is the interplay between these parameters that produces the resulting rich and complex dynamics at the network scale. The dynamics are sufficiently complex that it is not currently possible to theoretically predict the temporally evolving behavior of the network. Consequently, determining at an arbitrary time T_o whether the dynamics will saturate (become epileptic) or quiescent requires observation of all nodes in the network.

In the remainder of this section, we provide a self-contained technical description of the model. Readers interested in its full development, associated proofs, and theoretical and experimental results are referred to the references listed below.

3.1 The Refraction Ratio and its Effects on Dynamics

We first motivate the model and the network dynamic problem by presenting a simple but powerful example of how network geometry and signal latencies impact dynamics when coupled with the internal processing time of signals by individual nodes, manifested as a refractory period.

A critical theoretical result of our work is the derivation of what we term the *refraction ratio*. We have demonstrated mathematically (via formal proofs) that the refraction ratio imposes physical constraints on the optimal conditions for dynamic activity in networks with a physical structural geometry [8]. Brain networks fall into this category and are subject to these constraints. Specifically, the ratio between the distances signals must travel within the convoluted geometry of the network, and the speed at which they propagate must be carefully balanced with the time individual nodes require to process incoming information. This balance ensures coherent network dynamics. This concept is independent of scale, so it applies equally to networks of connected neurons in a particular circuit in a part of the brain as it does to connected brain regions at the scale of the whole brain. The refraction ratio encapsulates this relationship by balancing

- i. *Local constraints*: The time each node requires to process information internally.
- ii. *Global constraints*: The time required for signals to traverse the network as a function of its geometry and signaling speeds (conduction velocities).

An example of the effect of deviations from an optimized refraction ratio is shown in Figure 1. This example involves a simulated neurobiological network of 100 neurons modeled as Izhikevich neurons [9], a simplified mathematical representation of Hodgkin-Huxley neurons. Raster plots, commonly used by neuroscientists to visualize neural activity, illustrate the dynamics of the entire network. The vertical axis enumerates each neuron from 1 to 100, while the horizontal axis represents time, in this example spanning 4 seconds (4000 milliseconds). A tick mark along the time axis for a given neuron indicates that the neuron fired (an action potential) at that time.

This network is geometric, meaning the physical distance between neurons influences dynamics (Figure 1A and B). Specifically, signal propagation speeds — action potential conduction velocities — over these distances introduce latencies (or delays). Additionally, each neuron has a refractory period, during which it cannot respond to other incoming signals.

In this example, the network was externally stimulated for the first 500 milliseconds. We then assessed its ability to sustain inherent recurrent signaling without additional external stimulation. The network exhibited recurrent, low-frequency, periodic sustained activity at the lowest signaling speed (Figure 1C top panel). However, when the signaling speed was increased by a factor of 100, no activity persisted beyond the externally driven stimulus period; all activity ceased (Figure 1C bottom panel).

This cessation was the result of a mismatch in the refraction ratio. When signals arrived too quickly, neurons could not recover from their refractory periods. Consequently, incoming signals failed to induce downstream activations, and the activity in the network collapsed entirely.

3.2 Prior Work

The main theoretical results, including proofs and derivations, can be found in [8]. These results build on earlier findings that extended the modeling of biological geometric neural networks and their dynamics [7].

We have demonstrated that at least one class of neurons — basket cell inhibitory neurons in the cortex — has evolved specific morphological features to optimize the refraction ratio as an optimization principle, as a result enhancing signaling efficiency [10]. Additionally, the neurobiological connectome of the worm

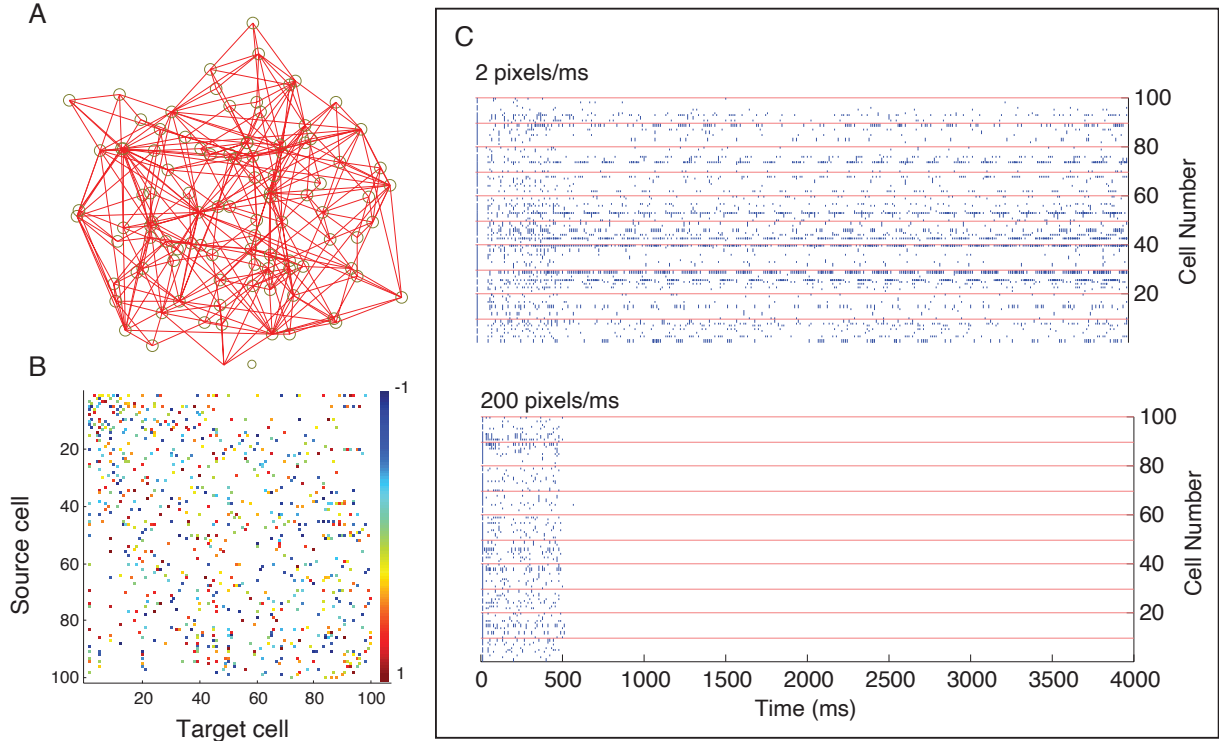


Figure 1: Effects of signaling speed (conduction velocities) and resultant latencies on the dynamics of a geometric neural network with neuronal (node) refractory periods. A. Graphical representation of the spatial locations of nodes and their physical (structural) connectivity in the plane. B. Functional connections were assigned random weights uniformly between -1 and 1 on each physical edge. An Izhikevitch model of bursting neurons was used to model the individual vertex dynamics. C. When the conduction velocities of signal propagation's was varied, the signaling delay distribution (temporal latencies) scaled and had a significant impact on the spike train dynamics (see text). Adapted from [7].

C. elegans leverages the refraction ratio and refractory dynamics to optimize signaling and coordinate motor outputs [11]. This model has also been adapted for use in a novel machine learning data embedding method [12, 13].

Our most recent (unpublished) data, collected using magnetoencephalography (MEG) in humans, further suggests that a form of the refraction ratio preserves perceptual symmetries during intra- versus inter-hemispheric visual tasks. These findings underscore the model’s broad applicability and relevance to biological and artificial neural network systems.

In the remainder of this section, we discuss the mathematical construction of the model and the refraction ratio, focusing on how fractional signaling summations produce activation event outputs. This aspect directly relates to the problem we address in this paper and its mapping to the quantum domain. However, we do not explore how the refraction ratio produces theoretical bounds on efficient network signaling, which is less important to the work in this paper. We also do not provide proofs for the stated theorems. Interested readers are referred to the cited references for a more comprehensive treatment.

3.3 Mathematical Introduction to the Model

The model describes how temporal latencies create offsets in the timing of summations for incoming discrete signaling events, such as neuronal action potentials, and how these interactions lead to the activation of downstream nodes. It captures how the timing of different signals compete to activate the nodes they arrive at. Here, *activation* refers to the appropriate reaction of a node to incoming signals. For biological neurons, this usually means generating an action potential that propagates down the axon and its axonal arborizations to downstream synapses. This is followed by a period of refractoriness, during which the neuron cannot respond to new incoming action potentials.

In a more abstract sense, the concept of activation generalizes to the production of discrete signaling events appropriate to the network (e.g., excitatory versus inhibitory), and refractoriness generalizes to the information processing time of a node required for its internal computations to result in an actionable computational output. The interplay between the temporal latencies of propagating discrete events across the network and the internal dynamics of individual nodes profoundly influences the overall network behavior, as demonstrated above in section 3.1.

In a geometric network, temporal latencies arise from the interplay between the signaling speeds and the geometry of the network’s edges, i.e., the path lengths between connected nodes. The model assumes that each node has an associated *refractory period* or *refractory state*, which reflects its internal state after activation by an upstream node (or set of nodes). The node cannot respond to other incoming signals during this refractory period. We make no assumptions about the internal model producing this refractory state, which could include an internal processing period during which the node decides how to react or could be due to the physical makeup and operation of the node, or both. For example, in biological neurons, the biophysics associated with the molecular resetting of sodium ion channel inactivation domains determines the absolute refractory period.

3.3.1 Geometric network construction

The model considers a spatial-temporal network where signals propagate between nodes along directed edges at a finite speed or conduction velocity, resulting in temporal delays (latencies) in signal arrival. These latencies naturally map a geometric representation of the network, where each node can be assigned a spatial position in \mathbb{R}^3 for every vertex v_i , with $i = 1, \dots, N$, where N is the number of nodes in the network, or its size. We use the terms *vertices* and *nodes* interchangeably.

Edges between nodes can follow convoluted paths, reflecting the physical geometry of connections. A signaling latency τ_{ij} is defined as the ratio between the distance traveled on an edge, $d_{ij} = |e_{ij}|$, and the speed of the propagating signal, s_{ij} :

$$\tau_{ij} = \frac{d_{ij}}{s_{ij}}.$$

The set of all edges in the network graph $G = (V, E)$ is denoted by $E = \{e_{ij}\}$, where e_{ij} represents the directed edge from vertex v_i to vertex v_j . The set of all vertices is given by $V = \{v_j\}$ for $j = 1, 2, \dots, N$ for a graph of size N vertices. We define the subgraph H_j as the (inverted) tree graph consisting of all vertices v_i with directed edges into v_j . In other words, this represents the subgraph of all incoming directed connections into v_j .

We write $H_j(v_i)$ to denote the set of all vertices v_i in H_j , and $H_j[v_i]$ to refer to a specific $v_i \in H_j(v_i)$. Signals traveling on the edges e_{ij} propagate at finite speeds s_{ij} , where $0 < s_{ij} < \infty$. As a first approximation, we assume that a single arriving discrete signal has the potential to activate v_j . To indicate causality, we use the notation $H_j[v_i] \rightsquigarrow v_j$ to signify that vertex $v_i \in H_j(v_i)$ causally activates v_j , meaning that v_i is the *winning* vertex whose signal successfully activates v_j . We first treat and analyze this restricted (single activation) case and 3.3.3) and then generalize the model to a latency-determined spatial-temporal version of a perceptron that activates due to the fractional summation of many arriving discrete signals (section 3.5.3).

3.3.2 Refractory period and signal dynamics

Each node v_j is assigned an *absolute refractory period*, given by R_j , which represents the amount of time the node requires for its internal dynamics to decide its output after being activated. Alternatively, R_j can also reflect a reset period during which v_j cannot respond to subsequent incoming signals.

We impose no restrictions on the internal processes or models that produce R_j . But we assume that R_j can be observed or measured and that $R_j > 0$ (i.e., recovery is never instantaneous, though it may be arbitrarily short). This assumption is reasonable for any physically realizable network.

Consider a vertex v_i with a directed edge e_{ij} connecting to a vertex v_j . For v_i to signal v_j , a discrete signal must propagate along e_{ij} at a finite speed s_{ij} . While s_{ij} could be constant for all edges, this is not required in the general case. Similarly, while nodes in the network may share the same refractory period (i.e., $R_j = R \forall v_j \in V$), the framework accommodates node-specific values of R_j .

If v_j is activated due to a signal from one of the v_i nodes connected into v_j , it becomes refractory for a period R_j , during which it cannot respond to additional incoming signals. The temporal nature of R_j implies that as time progresses, R_j gradually decreases and eventually decays to zero, at which point v_j can respond to a new input.

3.3.3 Internal dynamics of v_j

Let $f_j(\Omega_j, t)$ represent the instantaneous state of a vertex v_j as a function of time and an internal node model or activation function with parameter set Ω_j . Informally, the internal state can be interpreted as a binary function, which we define at an observation time T_o as:

$$f_j(\Omega_j, T_o) = \begin{cases} 1, & \text{if } v_j \text{ can respond to an input,} \\ 0, & \text{if it is refractory to any input.} \end{cases} \quad (1)$$

In the simpler single activation case, we assume that the first arriving discrete signal from any of the v_i vertices connected into v_j can activate it. Once this occurs, v_j becomes refractory for a duration R_j , during which $f_j = 0$. Below, we will progressively build out more neurobiologically realistic conditions (that do not rely on just one signaling event activating v_j), and we will formalize what we mean by 'can respond to an input' and 'is refractory to an input'.

3.3.4 Refraction ratio and signal competition

To compute, in parallel, which vertex $v_i \in H_j(v_i)$ causally activates v_j at discrete times, i.e., $H_j[v_i] \rightsquigarrow v_j$ in the notation we established above, we track the 'position' of propagating signals along edges, and therefore the amount of latency before they reach target vertices, relative to the refractory states of vertices. This is achieved using the *refraction ratio*, defined as the ratio between the refractory period R_j and the signaling latency τ_{ij} associated with a discrete signal from vertex v_i to v_j :

$$\Delta_{ij} = \frac{R_j}{\tau_{ij}} = \frac{R_j \cdot s_{ij}}{d_{ij}}. \quad (2)$$

This ratio provides a basis for computing and determining $H_j[v_i] \rightsquigarrow v_j$ by analyzing Δ_{ij} for all $v_i \in H_j(v_i)$.

3.3.5 Bounds and constraints on Δ_{ij}

We assume several physical constraints inherent to real-world networks that, as a result, impose bounds on Δ_{ij}

- i As $R_j \rightarrow 0$, $y_j = 1$ at all times, implying an instantaneous recovery from refractoriness, which is physically unrealizable. Hence, $R_j > 0$.
- ii As $R_j \rightarrow \infty$, $y_j = 0$ at all times, resulting in no information flow or signaling. Thus, $0 < R_j < \infty$.
- iii As $\tau_{ij} \rightarrow 0$, Δ_{ij} becomes undefined, corresponding to $d_{ij} \rightarrow 0$ (zero edge length) or $s_{ij} \rightarrow \infty$ (instantaneous signaling), which are unattainable conditions.

Thus, Δ_{ij} is restricted to finite signaling dynamics consistent with physical constraints.

3.3.6 Effective refractory period and temporal offsets

If v_j becomes refractory before an arbitrary observation time T_o , it could be in this state for a residual time less than R_j at T_o . For example, if v_j is halfway recovered from its refractory period at the time the node is observed at T_o , then the remaining amount of time before it can be activated again will be $R_j/2$, and not the full period R_j . This requires accounting for 'how much time is left' in both the signaling latencies τ_{ij} and the refractory periods R_j at T_o to compute activation patterns. We define the residual refractory period at T_o as the *effective refractory period*, denoted \bar{R}_j , which is central to our model.

We define the effective refractory period \bar{R}_j as:

$$\bar{R}_j = R_j - \phi_j, \quad \text{where } 0 \leq \phi_j \leq R_j. \quad (3)$$

Here, ϕ_j is the temporal offset from R_j at T_o :

- i. $\phi_j = 0$ implies that v_j becomes refractory exactly at T_o .

- ii. $\phi_j = R_j$ will occur only when v_j is fully recovered and responsive to any input.
- iii. $0 < \phi_j < R_j$ implies that v_j is partially recovered but not yet fully responsive.

Similarly, the signaling latency τ_{ij} is modified relative to T_o due to temporal offsets in signal propagation. This occurs because recall that by definition τ_{ij} is the *total* time it takes a signal to travel from node v_i to the target node v_j . Any signal that is partially along its way at T_o will take less time, and any signal that initiates after T_o is effectively elongated, i.e., takes longer to arrive at v_j . We define the *effective latency* as:

$$\bar{\tau}_{ij} = \tau_{ij} + \delta_{ij}, \quad \text{where } \delta_{ij} \in \mathbb{R}. \quad (4)$$

- i. $\delta_{ij} > 0$ encodes a delay in signaling initiation after T_o .
- ii. $-\tau_{ij} < \delta_{ij} < 0$ will result when a signal partially travels along e_{ij} prior to T_o .
- iii. $\delta_{ij} = 0$ implies a signal initiation occurs exactly at T_o .

3.3.7 Extended refraction ratio

We can now extend the refraction ratio to incorporate effective refractory periods and effective latencies as

$$\Lambda_{ij} = \frac{\bar{R}_j}{\bar{\tau}_{ij}}. \quad (5)$$

Including temporal offsets produces a huge combinatorial solution space for determining activation patterns of v_j , although a systematic investigation of this space is beyond the scope of this paper. The global dynamics of the network emerge from the local, statistically independent dynamics of each vertex and its subgraph $H_j(v_i)$. Once v_j is activated, it contributes to the activation dynamics of downstream vertices it connects to, contributing, in turn, to the network's dynamic behavior.

3.4 Analysis of Activation Conditions

Intuitively, the *activation* vertex $v_i \in H_j(v_i)$ that successfully activates v_j , i.e., $H_j[v_i] \rightsquigarrow v_j$, will correspond to the first signaling event to arrive at v_j immediately after v_j ceases to be refractory. This is equivalent to stating that $H_j[v_i] \rightsquigarrow v_j$ will be achieved by the v_i with the smallest value of $\bar{\tau}_{ij}$ greater than \bar{R}_j . This condition ensures activation and can be expressed as $\bar{\tau}_{ij} \rightarrow \bar{R}_j^+$, i.e., $\bar{\tau}_{ij}$ approaches \bar{R}_j from the right. Determining this condition requires computing the order of arriving signaling events, effectively implementing an algorithm to compute $H_j[v_i] \rightsquigarrow v_j$ at T_o .

To formalize this, we first define a well-ordered set of refraction ratios (in a set-theoretic sense), Λ_{ij} . We then consider the condition $\bar{\tau}_{ij} \rightarrow \bar{R}_j^+$ and construct a subset whose elements contain only ratios that guarantee signal arrivals after refractoriness has completed:

$$\Lambda_{ij}^o := \{\Lambda_{ij} : i = 1, 2, \dots, N \mid \bar{\tau}_{ij} \rightarrow \bar{R}_j^+\}. \quad (6)$$

This implies that every $\Lambda_{ij} \in \Lambda_{ij}^o$ satisfies $\Lambda_{ij} < 1$, which follows from the definition of the ratio in equation 5, where the refractory period is in the numerator and the latency is in the denominator.

We impose a structure on Λ_{ij}^o by ordering it with the standard $>$ operator, arranging the ratios from largest to smallest. Since H_j is finite, consisting of a finite number of v_i vertices connecting into v_j , Λ_{ij}^o is also a finite set. Using Λ_{ij}^o , we compute $H_j[v_i] \rightsquigarrow v_j$ as follows.

3.4.1 Theorems for determining activation vertices

Theorem 1. Assume vertex v_j has an effective refractory period \bar{R}_j at observation time T_o . If $\phi_j \neq R_j$, then the condition $H_j[v_i] \rightsquigarrow v_j$ is given by the refraction ratio $\Lambda_{ij} \in \Lambda_{ij}^o$ that satisfies:

$$v_i = \lceil \max(\Lambda_{ij}) \rceil. \quad (7)$$

If, on the other hand, $\phi_j = R_j$, the condition $H_j[v_i] \rightsquigarrow v_j$ is determined by:

$$\min(\bar{\tau}_{ij}) \quad \forall v_i \in H_j(v_i). \quad (8)$$

Alternatively, Theorem 1 can be expressed equivalently as:

Theorem 2. Assume vertex v_j has an effective refractory period \bar{R}_j at observation time T_o . For each $v_i \in H_j(v_i)$ with associated $\bar{\tau}_{ij}$, the condition $H_j[v_i] \rightsquigarrow v_j$ is satisfied by:

$$\min [(\bar{\tau}_{ij} - \bar{R}_j) > 0]. \quad (9)$$

Algorithmically, equation 9 is more efficient to implement, as it requires computing a simple difference rather than a ratio. This efficiency becomes significant when determining all $H_j \in G(V, E)$ in parallel in a network. Proofs for these theorems can be found in [8].

3.5 Extensions Beyond the Basic Construction

In this section, we summarize several natural extensions of the basic single-activation construction. These extensions improve the neurobiological realism and applicability of the model. We first introduce a probabilistic version of the framework, reflecting the stochastic nature of generating action potentials and associated biological processes. We then discuss an approach for handling inhibitory inputs and their impact on network dynamics. Finally, we summarize a version of the framework that incorporates fractional contributions from summing signals. This addition effectively represents a geometric dynamic extension of the classical perceptron model. It is important to note that these extensions are not mutually exclusive. The framework can be implemented to simultaneously accommodate any or all of these extensions, further enriching the model's dynamic complexity and functional capacity.

3.5.1 Probabilistic extension

As developed in the preceding sections, the framework is deterministic, meaning that a single vertex v_i is guaranteed to activate v_j when the condition $H_j[v_i] \rightsquigarrow v_j$ is satisfied. In other words, the probability of v_j responding to a *winning* signal from v_i is exactly 1. However, biological neural networks are not deterministically precise and are often influenced by random fluctuations in signaling processes. These fluctuations may arise due to thermal dynamics, sub-diffusion processes, or molecular stochasticity, such as neurotransmitter vesicles crossing the synaptic cleft or the probabilistic binding of neurotransmitters on the postsynaptic membrane.

We define a probability distribution P_{ij} to represent the likelihood that a winning vertex $H_j[v_i] \rightsquigarrow v_j$ successfully activates v_j . Let $v_j(P_{ij})$ denote the output probability of v_j for a given threshold $P_{threshold}$. The activation condition for v_j based on P_{ij} can then be defined as:

$$v_j(P_{ij}) = \begin{cases} 1, & \text{if } H_j[v_i] \rightsquigarrow v_j \text{ and } P_{ij} \geq P_{threshold}, \\ 0, & \text{if } H_j[v_i] \rightsquigarrow v_j \text{ and } P_{ij} < P_{threshold}. \end{cases} \quad (10)$$

It is important to note that equation 10 does not specify the exact nature of v_j 's output when $v_j(P_{ij}) = 1$. This could result in a signal being generated if v_i is excitatory or no signal if v_i is inhibitory (see Section 3.5.2). The equation solely indicates that v_j *responds* in some manner to v_i 's signal appropriate to the behavior of that class of node.

3.5.2 Inhibitory inputs into v_j

The framework can also accommodate inhibitory inputs in the following manner: If an *activation* vertex v_i satisfies $H_j[v_i] \rightsquigarrow v_j$, then:

- i. If the input from v_i is excitatory, v_j generates an output signal and becomes refractory for a duration \bar{R}_j .
- ii. If the input from v_i is inhibitory, v_j does not generate an output signal but becomes refractory for \bar{R}_j .

In the inhibitory case, the absence of an output from v_j prevents its contribution to the activation of its downstream vertices while ensuring that v_j remains unable to respond to further inputs until its refractory period ends.

This approach to modeling excitatory and inhibitory inputs is straightforward and computationally efficient, though other methods for differentiating between input types could be considered.

3.5.3 Fractional summation of contributing signaling events

In this section, we describe an extension of the framework that incorporates the summation of fractional contributions from multiple nodes towards activating a vertex v_j . Instead of a single node v_i solely deterministically or probabilistically activating v_j , we consider what happens when we have a *running summation* of contributions from multiple $v_i \in H_j(v_i)$ that collectively need to reach a threshold Σ_T to activate v_j . Once v_j fires, it becomes refractory, as described above.

Conceptually, this extension represents a geometric refractory model of the classical perceptron, where the signaling latencies and geometric considerations of the network play a critical role in determining activation. These perceptrons can be envisioned as having a geometric morphology that accounts for computed latencies along edges (inputs into v_j), similar to biological neurons. The interplay between the latencies of discrete signals, the evolving refractory state of v_j , and the decaying contributions of weights determines the dynamic summation towards threshold.

We assume weights and an activation function as in the standard perceptron model. Additionally, we introduce a *decay function* to provide a memory or history for previous signals. This function assigns diminishing but non-zero contributions to the summation from inputs that arrived before the observation time T_o . As such, the computational goal is no longer to predict which $v_i \in H_j(v_i)$ will activate v_j , but rather which *subset* of $H_j(v_i)$ will collectively do so.

Running summation towards threshold. Assume an observation time T_o , and let v_j be non-refractory. The running summation Σ_r from $H_j(v_i)$ must reach a threshold Σ_T for v_j to activate at some $t \geq T_o$. Upon activation, v_j becomes refractory for a period R_j . The specific contribution from each $v_i \in H_j(v_i)$ is given by a weight w_{ij} , representing synaptic strength. While not strictly necessary, we assume the added condition that Σ_T is constant for all $v_j \in V$.

We assume a set of weights $W_j = \{w_{ij}\}$ for all connections into v_j . The maximum weight $w_{ij,max}$ occurs when the signal from v_i first arrives at v_j while it is non-refractory, i.e., at $(\bar{\tau}_{ij} - \bar{R}_j)$ (c.f. Theorem 2).

After arrival, we assume a time-varying weight $w_{ij}(t)$ whose contribution decays over time, such that:

$$w_{ij}(t) < w_{ij,max} \quad \text{for } t > (\bar{\tau}_{ij} - \bar{R}_j).$$

This finite memory models the progressively diminishing impact of prior signals.

Incorporating decay dynamics. We then need to define a decay function $D_i(t)$ that modulates each weight after its corresponding signal arrives. This ensures that more recent arriving signals contribute more to the running summation than prior signals. At the moment a signal from v_i arrives at v_j , the decay function satisfies:

$$D_i(\bar{\tau}_{ij} - \bar{R}_j) = 0, \quad (11a)$$

$$D_i[(\bar{\tau}_{ij} - \bar{R}_j) + \xi] = 1, \quad (11b)$$

where ξ represents the decay duration. For intermediate times:

$$\begin{aligned} &\text{If } (\bar{\tau}_{ij} - \bar{R}_j) < t < (\bar{\tau}_{ij} - \bar{R}_j) + \xi, \\ &\text{then } D_i(t_n) < D_i(t_m) \quad \text{for } t_n < t_m. \end{aligned} \quad (12)$$

The decay function $D_i(t)$ is strictly increasing, ensuring a progressive reduction in the contribution of w_{ij} . The decayed weight is given by:

$$w_{ij}(t) = w_{ij,max} - w_{ij,max} \cdot D_i(t), \quad (13)$$

where the domain of $D_i(t)$ is $(\bar{\tau}_{ij} - \bar{R}_j) \leq t \leq (\bar{\tau}_{ij} - \bar{R}_j) + \xi$, and its codomain is $0 \leq D_i(t) \leq 1$.

Summation with decaying contributions. To compute the fractional contributions of weights towards Σ_r , consider the subset $\Lambda_M \subset \Lambda_{ij}^o$, where:

$$\Lambda_M = \{(\Lambda_{ij})_m \in \Lambda_{ij}^o : m = 1, 2, \dots, M\}.$$

This subset is the set of M signals (as refraction ratios) that arrive after v_j has recovered from its refractory period that contribute to the running summation that gets v_j to its next activation (firing) state.

The running summation of the maximum weights that contribute to getting v_j to its threshold is:

$$\Sigma_r = \sum_{m=1}^M (w_{ij,max})_m \geq \Sigma_T. \quad (14)$$

To account for weight decays as defined above, we compute the fractional contribution of each weight at the moment $t = (\bar{\tau}_{Mj} - \bar{R}_j)$ when threshold is reached:

$$\Sigma_r = \sum_{m=1}^M [(w_{ij,max})_m - (w_{ij,max})_m \cdot D_i(\bar{\tau}_{Mj} - \bar{\tau}_{ij})] \geq \Sigma_T. \quad (15)$$

Here, $D_i(\bar{\tau}_{Mj} - \bar{\tau}_{ij})$ reflects the decay function's value at the time difference between signal arrival and threshold activation. Excitatory and inhibitory inputs can be incorporated as described in Section 3.5.2, where inhibitory weights contribute negatively to Σ_r . Note that in computing equation 15, transient computations (e.g., weight decay levels and signaling latencies) do not necessarily need to be stored long-term.

This reduces the computational overhead and memory and storage requirements if the evolving dynamics do not need to be measured or visualized until T_o .

With the model now fully developed, we can revisit the condition for the state of node v_j , given by f_j , as informally introduced in equation 1. The state of v_j at an arbitrary observation time T_o is given by

$$F(V, T_o) := f_j(T_o) = \begin{cases} 1 & \text{if } \Sigma_r \geq \Sigma_T, v_j = 1 \\ 0 & \text{if } \Sigma_r < \Sigma_T, v_j = 0 \end{cases} \quad (16)$$

Determining the state given by equation 15 for every node in the network by computing equation 15 in parallel at an observation or measurement time T_o defines the network dynamical state at T_o .

Assuming an excitatory network, i.e., a network where for all nodes if a node is activated it generates an excitatory output, we are now in a position to formally restate the key question we ask in this paper: Given some (observed or unobserved) period of evolution dynamics of a network computed by equation 15, can the dynamics (state) of the network sustain inherent activity beyond an arbitrary observation time T_o , or are the dynamics guaranteed to stop, either due to 'epileptic'-like saturation or quiescence? The (global) state of the network is determined by $F(V, T_o) = f_j(T_o) \forall v \in V$ (equation 16).

4 Preparing Network States for Deutsch-Jozsa Computations

To leverage the Deutsch–Jozsa algorithm, we need to structure the problem so that it naturally exploits the algorithm's deterministic superposition properties. This will allow us to determine the global state of the network all at once, rather than needing to classically compute and check the state of every v_j individually.

To achieve this, we will first construct a specific set that encodes the states of $v_j \in V$. When presented as an input to Deutsch–Jozsa, the output can be interpreted as an answer to the question about the network's dynamics. We will also use Grover's algorithm to evaluate set membership within this framework.

4.1 Set Membership Conditions

Each vertex $v_j \in V$ is associated with a value $\Sigma_r \in \mathbb{R}$ at time T_o , that is typically normalized to a defined range:

$$\epsilon \leq \Sigma_r \leq (\epsilon + \Delta),$$

commonly within $0 \leq \Sigma_r \leq 1$.

This range can be approximated by an n -bit string representation with sufficient precision:

$$\Sigma_r \in \{0, 1\}^n.$$

For the remainder of the paper, Σ_r will refer to this n -bit string representation. We do not need to distinguish between the n -bit string and continuous numerical representations in the notation.

In this context, $F(V, T_o)$ is a function that compares the n -bit input Σ_r , the running summation for each vertex $v_j \in V$, to a constant threshold $\Sigma_T \in \{0, 1\}^n$ (equation 16). To determine the global state of the network, we evaluate $F(V, T_o)$ for all $v_j \in V$ at time T_o , where the output is either 0 or 1 for each node, indicating whether v_j fires (activates) at the next time step (c.f. Section 3.5.3).

For realistic networks, both biological and artificial, the cardinality of V , $|V| = N$, may be very large. However, the set of Σ_r values is much smaller. Given an n -bit precision to represent Σ_r , many nodes may share the same Σ_r values, while some values of Σ_r may appear uniquely only once, and others may not occur at all. Thus, only a subset of the possible n -bit strings representing the full set of possible values of Σ_r may be realized during the network's dynamics.

Mathematically, we construct an ordered list \mathbb{V} such that its elements map each vertex $v_j \in V$ to its corresponding value of Σ_r :

$$\mathbb{V} : v_j \rightarrow \Sigma_r \quad \forall v_j \in V. \quad (17)$$

To formalize this, let \mathbb{S}_n denote the set of all possible n -bit strings:

$$\mathbb{S}_n := \{s_i \mid s_i \in \{0, 1\}^n\}. \quad (18)$$

We then define the following subsets:

- i. S_n is the subset of \mathbb{S}_n that represents all n -bit string values of Σ_r that occur in the network up to the observation time T_o , i.e. values of $\Sigma_r \in \mathbb{S}_n$ that are actually realized:

$$S_n := \{s_i \mid s_i \in \mathbb{S}_n \wedge s_i = \Sigma_r \in \mathbb{V}\}. \quad (19)$$

- ii. S_n^c is the complement of S_n , containing all n -bit strings that do not represent values of Σ_r :

$$S_n^c := \{s_i \mid s_i \in \mathbb{S}_n \wedge s_i \neq \Sigma_r \in \mathbb{V}\}. \quad (20)$$

Clearly, $S_n \cup S_n^c = \mathbb{S}_n$.

There exists a surjective mapping $\mathbb{V} \rightarrow \mathbb{S}_n$: Each $v_j \in V$ maps to one of the n -bit string values $s_i \in \mathbb{S}_n$. In general, we expect:

$$|\mathbb{V}| = |V| = N > |\mathbb{S}_n| \geq |S_n|.$$

For instance, while $|V|$ may be in the millions or billions, representing Σ_r to two decimal places requires only 7 bits, encoding 128 values. This includes 101 values from 0.00 to 0.99 and the value 1.00.

Given this construction, another canonical quantum computing algorithm, Grover's algorithm, can determine set membership in S_n . The interpretation of S_n in the context of how the question about neural dynamics is framed motivates the construction of the unitary function to be evaluated by the Deutsch–Jozsa algorithm later on.

4.2 Functional Interpretations of $F(V, T_o)$ Outcomes

Recall that our goal is to determine if the network's dynamics can sustain inherent activity beyond T_o , or whether it is guaranteed to stop due to either 'epileptic' saturation or quiescence. This is achieved by evaluating the global state of the network using $f_j(T_o)$.

- i. *Epileptic saturation* is a state where all neurons in the network fire simultaneously at T_o , characterized by

$$F(V, T_o) = f_j(T_o) = 1 \quad \forall v_j \in V$$

- ii. *Quiescence* is a state where no neurons fire, implying no further activity without external input, which occurs when

$$F(V, T_o) = f_j(T_o) = 0 \quad \forall v_j \in V$$

In both cases, $F(V, T_o)$ is constant (in the language of Deutsch–Jozsa), mapping S_n to binary outputs $\{0, 1\}$. In contrast, *inherent dynamic activity* will occur only when $F(V, T_o)$ is *not* constant, which we can interpret as the network being able to sustain autonomous activity for at least one additional time step.

By running the Deutsch–Jozsa algorithm twice, we can distinguish between constant and non-constant states of $F(V, T_o)$. A non-constant result implies that the network is neither epileptic nor quiescent. It is important to note that $F(V, T_o)$ need not be balanced — only not constant. This agrees with the Deutsch–Jozsa requirement for unitary functions of the form $f(\{0, 1\}^n) \rightarrow \{0, 1\}$.

It is *critical* to note in the statement above that this is a special use case of the Deutsch–Jozsa algorithm. Deutsch–Jozsa takes as input a function that evaluates a binary sequence of 0's and 1's, i.e., a set $\{0, 1\}^n$, and uses quantum superposition to simultaneously determine if the input function's output is *constant* (all 0's or all 1's) or whether the output is *balanced* (an equal number of 0's and 1's). To evaluate $F(V, T_o) = F(S_n)$ using Deutsch–Jozsa, we first need to extend S_n to a construction compatible with the algorithm. In our case, we need to evaluate S_n as inputs and not the full domain $\mathbb{S}_n = \{0, 1\}^n$. Deutsch–Jozsa assumes that the oracle function being evaluated is defined over the entire domain \mathbb{S}_n . It cannot evaluate a particular subset of $\{0, 1\}^n$. Thus, it cannot explicitly evaluate $F(V, T_o) = F(S_n)$. We show how to carry this out below.

4.3 Determining Membership in S_n and S_n^c Using Grover's Algorithm

To identify which elements of \mathbb{S}_n belong to S_n , we need to search for each n -bit string $s_i \in \mathbb{S}_n$ that is in the list \mathbb{V} , which contains the values of Σ_r resulting from the dynamic evolution of the network up to the observation time T_o . The resultant set is S_n , and its complement in \mathbb{S}_n forms S_n^c . Recall that we expect some elements of \mathbb{S}_n to appear in \mathbb{V} only once, some multiple times, and others not at all. Grover's algorithm offers a potential quadratic speedup over classical approaches to construct S_n by enabling an efficient search within \mathbb{S}_n .

4.3.1 Construction of the oracle function

The list \mathbb{V} contains the running summation values Σ_r for each vertex v_j at T_o (see equation 17). Assume each element in \mathbb{V} is labeled as $\{\nu_1, \nu_2, \dots, \nu_M\}$. Each of these elements of \mathbb{V} corresponds to an n -bit string in \mathbb{S}_n . For each $s_i \in \mathbb{S}_n$, we construct an oracle function U_f to identify if $s_i \in \mathbb{V}$. Specifically, U_f checks if there exists a $\nu_i \in \mathbb{V}$ such that $\nu_i = s_i$ for some $s_i \in \mathbb{S}_n$:

$$\exists \nu_i \in \mathbb{V} \text{ such that } \nu_i = s_i. \quad (21)$$

The oracle function U_f performs the operation:

$$U_f |\nu_i\rangle = (-1)^{f(\nu_i)} |\nu_i\rangle, \quad (22)$$

where $|\nu_i\rangle$ encodes a state corresponding to $\nu_i \in \mathbb{V}$, and $f(\nu_i)$ evaluates to 1 if $\nu_i = s_i$, and 0 otherwise.

To construct U_f , a programmable oracle function will be required on a physical machine capable of implementing the logical condition ‘if the current state $\nu_i = s_i$, apply a phase flip; otherwise, do nothing’. This could be achieved through conditional quantum gates for each s_i . The technical and hardware implementations to achieve this carry their own challenges. Our focus in this paper, however, is on the theoretical and algorithmic constructions and considerations of the problem setup and solution. We leave a discussion about the possible approaches to the physical computation of the theoretical structures we derive in this section and the rest of the paper for future efforts.

4.3.2 Diffusion operator and search space

The standard diffusion operator D in Grover's algorithm is defined as:

$$D = 2|\sigma\rangle\langle\sigma| - I, \quad (23)$$

where $|\sigma\rangle$ is the uniform superposition over all $s_i \in \mathbb{S}_n$:

$$|\sigma\rangle = \frac{1}{\sqrt{N}} \sum_{s_i=0}^{N-1} |s_i\rangle. \quad (24)$$

Here, I is the $N \times N$ identity matrix, and $N = |\mathbb{S}_n| = 2^n$. The diffusion operator amplifies the amplitudes of marked states identified by U_f , inverting their amplitudes about the average. In our context, Grover's algorithm iteratively applies U_f and D to amplify the amplitudes of $s_i \in \mathbb{S}_n$ that are present in \mathbb{V} , which would allow efficient identification of elements in S_n .

4.3.3 Iterative application of Grover's algorithm

To determine membership of each $s_i \in \mathbb{S}_n$, the algorithm has to be run iteratively for each s_i . For example, continuing the example from above, a practically reasonable precision of Σ_r requiring at most 128 n -bit strings (7-bit precision) would involve $|\mathbb{S}_n| = 2^n \approx 10^2$ iterations.

In general, the number of iterations needed for amplitude amplification for a specific s_i is approximately

$$k \approx \frac{\pi}{4} \sqrt{\frac{N}{\mu}},$$

where μ is the number of occurrences of s_i in \mathbb{V} . The algorithm's efficiency improves with higher μ values because fewer iterations are required. For real physically constructable networks, there are likely other physical and functional constraints. So optimizing k may benefit from structural insights into $G(V, E)$, which could suggest and constrain patterns in \mathbb{V} . For example, signaling conditions that constrain the possible range of values Σ_r can take.

In the worst case, the algorithm requires approximately $\frac{\pi}{4} \sqrt{N}$ iterations, yielding a quadratic speedup over classical search methods, which would require $O(N)$ steps to evaluate each s_i sequentially.

4.3.4 Probabilistic nature and verification

If the algorithm identifies $s_i \in \mathbb{V}$ once measured, we assume it is part of S_n . If the algorithm returns $s_j \neq s_i$, we conditionally assume $s_i \notin \mathbb{V}$. However, there is a non-zero chance of error because of the probabilistic nature of quantum mechanics. In a practical sense, increasing the confidence of set membership may require re-running the algorithm for the same s_i .

Once S_n is identified, determining S_n^c is straightforward. It is simply the complement of S_n in \mathbb{S}_n : $S_n^c = \mathbb{S}_n \setminus S_n$. This allows us to construct both subsets efficiently using Grover's algorithm, setting up the computations we will do in the Deutsch–Jozsa computations.

5 Evaluating Network Dynamics with the Deutsch–Jozsa Algorithm

With S_n and S_n^c defined, we can now use the Deutsch–Jozsa algorithm to determine if the network can sustain inherent recurrent activity beyond T_o , or if its dynamics will necessarily cease. However, as discussed above, the evaluation must be done on S_n , a subset of $\mathbb{S}_n = \{0, 1\}^n$, rather than on the full domain.

To address this subset evaluation requirement, we extend S_n into \mathbb{S}_n by taking advantage of the relationship $S_n \cup S_n^c = \mathbb{S}_n$. This construction will let us interpret the Deutsch–Jozsa algorithm’s output to indirectly infer the behavior of $f(S_n)$, as defined by equation 16. Here, $f(S_n)$ refers to the input function into the Deutsch–Jozsa algorithm, which, as required, is evaluated across the full domain \mathbb{S}_n . Specifically, the elements of S_n encode the key information about the network dynamics in the form of the node outputs at T_o (equation 16). As such, in our implementation here, $f(S_n)$ does not explicitly evaluate the elements of the input set S_n , but instead, it preserves them unchanged. It effectively acts as an identify function.

For elements in S_n^c , f does not evaluate their values explicitly. Instead, all elements of S_n^c are assigned a fixed value (either 0 or 1) for one algorithm run and then reassigned the other fixed value for a second subsequent run. This assignment ensures that we can infer the behavior of $f(S_n)$ based on the algorithm’s output. To do this, we need to construct and evaluate a two-part unitary function U_f across two distinct runs of the algorithm.

5.1 Evaluating S_n and S_n^c with a Two-Part U_f

We define a two-part oracle function U_f that operates on the composite state $|s_i\rangle|-\rangle$, where the ancillary qubit $|-\rangle$ is initialized as

$$|-\rangle = \frac{1}{\sqrt{2}}(|0\rangle - |1\rangle). \quad (25)$$

5.1.1 Behavior for S_n

For $s_i \in S_n$, the oracle function evaluates $f(s_i)$, flipping the phase of $|s_i\rangle$ when $f(s_i) = 1$ and leaving it unchanged when $f(s_i) = 0$, such that

$$\text{If } f(s_i) = 1 : \quad U_f |s_i\rangle|-\rangle = -|s_i\rangle|-\rangle, \quad (26a)$$

$$\text{If } f(s_i) = 0 : \quad U_f |s_i\rangle|-\rangle = |s_i\rangle|-\rangle. \quad (26b)$$

Note that for S_n , this computation will be the same for both runs of the algorithm.

5.1.2 Behavior for S_n^c

For $s_i \in S_n^c$, the oracle does not evaluate $f(s_i)$ directly. Instead:

- i. For the first run of the algorithm, all elements $s_i \in S_n^c$ are assigned $f(s_i) = 0$.
- ii. In a separate second run, all elements $s_i \in S_n^c$ are assigned $f(s_i) = 1$.

This ensures that S_n^c does not contribute to the dynamic information encoded in $f(S_n)$. But it satisfies the technical requirement that the input function $f(\cdot)$ operates over the entire domain \mathbb{S}_n by filling in the values of \mathbb{S}_n not encountered in S_n that encodes the dynamics.

Mathematically, for $s_i \in S_n^c$:

$$\text{If assigned } f(s_i) = 1 : \quad U_f |s_i\rangle|-\rangle = -|s_i\rangle|-\rangle, \quad (27a)$$

$$\text{If assigned } f(s_i) = 0 : \quad U_f |s_i\rangle|-\rangle = |s_i\rangle|-\rangle. \quad (27b)$$

5.2 Constructing U_f to Evaluate $f(S_n)$

To construct U_f , we need to combine two operations:

- i. Determination of set membership: Mark the elements of S_n^c so they are assigned fixed values without explicit evaluation (equation 27).
- ii. Evaluation of S_n : Apply $f(s_i)$ to elements in S_n according to equation 26.

The first step requires marking $s_i \in S_n^c$. This can be done using controlled phase-flip operations that selectively identify and act on states corresponding to S_n^c , leaving elements of S_n unchanged. These marking operations are performed in parallel across the superposition of S_n .

The second step evaluates $f(S_n)$ by comparing each Σ_r (encoded in s_i) with the threshold Σ_T . We implement this as a binary subtraction $\Sigma_r - \Sigma_T$, with the ancillary qubit encoding the result

- i. $|1\rangle$ if $\Sigma_r \geq \Sigma_T$, corresponding to $f(s_i) = 1$.
- ii. $|0\rangle$ if $\Sigma_r < \Sigma_T$, corresponding to $f(s_i) = 0$.

5.2.1 Example of a Binary Subtraction for Evaluating $f(S_n)$

Let's work through a specific example of a binary subtraction operation. Consider a vertex $v_j \in G(V, E)$ with a corresponding entry $\rho_i \in \mathbb{V}$ that encodes the running summation value Σ_r at the observation time T_o for the specific vertex v_j . Assume a 7-bit representation of Σ_r and the threshold Σ_T to two-decimal precision, as discussed in Section 4.1.

Let

$$|\rho\rangle = |1010101\rangle, \quad |\tau\rangle = |0110010\rangle.$$

where $|\rho\rangle$ encodes $\Sigma_r = 0.85$ in binary, while $|\tau\rangle$ encodes $\Sigma_T = 0.50$. The ancillary qubit, initially in state $|0\rangle$, will store the result of comparing $\Sigma_r \geq \Sigma_T$.

The binary subtraction operation is as follows:

$$\begin{array}{r} \rho = \begin{array}{ccccccc} 1 & 0 & 1 & 0 & 1 & 0 & 1 \end{array} \\ \tau = \begin{array}{ccccccc} 0 & 1 & 1 & 0 & 0 & 1 & 0 \end{array} \\ \hline \text{Result} = \begin{array}{ccccccc} 1 & -1 & 0 & 0 & 1 & -1 & 1 \end{array} \end{array}$$

Starting from the most significant bit, we compare ρ_6 to τ_6 . In this example, since $\rho_6 = 1 > \tau_6 = 0$, we can immediately determine that $\Sigma_r > \Sigma_T$ without needing to compare any other bits. If necessary, the comparison would progress to the next significant qubit until a determination is made. The consequence here is that the ancillary qubit is flipped to $|1\rangle$ to indicate that $f(s_i) = 1$.

In a physical quantum circuit this comparison can be implemented using a sequence of controlled gates that

- i. Compare corresponding bits ρ_i and τ_i sequentially from the most significant to least significant.
- ii. Stop and set the ancillary qubit when the first inequality $\rho_i > \tau_i$ is detected.

This binary subtraction comparison is efficient because it focuses only on detecting the sign of the result (i.e., positive or negative) rather than computing the full numerical value of $\Sigma_r - \Sigma_T$. Once $f(s_i)$ is computed for all $s_i \in S_n$, the Deutsch–Jozsa algorithm evaluates whether $f(S_n)$ is constant or not across the entire subset.

5.3 Measurement Interpretations of U_f

By running the Deutsch–Jozsa algorithm twice, assigning all elements of S_n^c first to $f(s_i) = 0$ and then to $f(s_i) = 1$, measurement outcomes provide an interpretation that answers our question about the network dynamics:

- i. **Quiescence:** If $S_n^c = 0$ and U_f evaluates to a constant state $|0\rangle^{\otimes n}$, the network is quiescent, because $f(S_n) = 0$ for all $s_i \in S_n$.
- ii. **Epileptic State:** If $S_n^c = 1$ and U_f evaluates to a constant state $|1\rangle^{\otimes n}$, the network is epileptic, because $f(S_n) = 1$ for all $s_i \in S_n$.
- iii. **Dynamic Activity:** If U_f is not constant for either case, we interpret this result as the network being able to potentially maintain inherent dynamic activity due to the measurement outcome reflecting what must be a mix of active and inactive vertices in S_n .

6 Comparative Algorithmic Complexity

This last section analyzes the algorithmic complexity of solving the problem using the Grover and Deutsch–Jozsa algorithms versus a purely classical approach. We will show that using these quantum algorithms conveys a significant computational advantage and speedup and demonstrate how such an advantage scales, i.e., becomes greater, as the size of the network being analyzed increases.

6.1 Classical complexity

Consider a network with $N = |V|$ vertices and let $S_n \subseteq \mathbb{S}_n$ represent the set of n -bit encodings of Σ_r , where $|\mathbb{S}_n| = 2^n$. A classical approach would need to

- i. Evaluate $F(V, T_o) = f_j(T_o)$ for each $v_j \in V$ in order to compare Σ_r and Σ_T (equation 16). This requires iterating over all vertices.
- ii. Combine the results of $f_j(T_o)$ for all $v_j \in V$ to determine whether the network is quiescent, epileptic, or dynamically active.

Assuming a binary comparison operation of complexity $O(n)$ for each v_j , the total complexity of the classical approach is

$$O_{\text{classical}} = O(N \cdot n).$$

6.2 Quantum complexity: Grover's algorithm

Grover's algorithm provides a quadratic speedup for searching an unstructured set. To determine S_n , we use Grover's algorithm to find all $s_i \in \mathbb{S}_n$ that belong to S_n . Let μ denote the number of occurrences of a particular s_i in \mathbb{V} , and $|\mathbb{S}_n| = 2^n$. The number of iterations required for Grover's algorithm to amplify the amplitude of each solution is approximately

$$k \approx \frac{\pi}{4} \sqrt{\frac{2^n}{\mu}}.$$

Assuming the worst case where $\mu = 1$, the complexity of finding each $s_i \in S_n$ is given by

$$O_{\text{Grover}} = O\left(2^{n/2}\right).$$

If S_n contains $|S_n|$ elements, the total complexity for constructing S_n is

$$O_{\text{Grover (total)}} = O\left(|S_n| \cdot 2^{n/2}\right).$$

6.3 Quantum complexity: Deutsch–Jozsa Algorithm

The Deutsch–Jozsa algorithm evaluates whether $f(S_n)$ is constant or not across all elements of \mathbb{S}_n . Unlike a classical approach that would require checking each $s_i \in \mathbb{S}_n$, the Deutsch–Jozsa algorithm achieves this in a constant number of evaluations:

$$O_{\text{Deutsch–Jozsa}} = O(1).$$

When combined with Grover's algorithm for constructing S_n , the total quantum complexity becomes

$$O_{\text{quantum total}} = O\left(|S_n| \cdot 2^{n/2} + 1\right).$$

6.4 Comparative analysis

As such, the task of evaluating $f(S_n)$ for all vertices in V can be summarized by

i. *Classical complexity*:

$$O_{\text{classical total}} = O(N \cdot n).$$

ii. *Quantum complexity*:

$$O_{\text{quantum total}} = O\left(|S_n| \cdot 2^{n/2} + 1\right).$$

For large N and n , a quantum algorithmic approach provides a significant increase in computational efficiency. Grover's algorithm provides a quadratic speedup in 2^n , while Deutsch–Jozsa evaluates $f(S_n)$ in constant time.

Let's consider a numerical example to illustrate this advantage. Consider a network with $N = 10^6$ vertices, where, as we have done throughout the paper, $n = 7$ bits are used to represent Σ_r with precision sufficient for two significant digits. This means that $|\mathbb{S}_n| = 2^n = 128$. Assume that $|S_n| = 100$.

For the **classical approach** each vertex requires $O(n) = O(7)$ steps for comparison. Evaluating all N vertices gives

$$O_{\text{classical total}} = O(10^6 \cdot 7) = O(7 \times 10^6).$$

For the **quantum approach**, using Grover to find all elements of S_n , with $|S_n| = 100$ and $|\mathbb{S}_n| = 128$ will require approximately

$$k \approx \frac{\pi}{4} \sqrt{\frac{128}{1}} \approx 11.3.$$

number of iterations. Thus, the total cost for Grover's step will be $O_{\text{Grover (total)}} = O(100 \cdot 11.3) \approx O(1130)$.

Then subsequently evaluating $f(S_n)$ with Deutsch–Jozsa adds a constant overhead of $O_{\text{Deutsch–Jozsa}} = O(1)$.

As a result, the total quantum complexity is given by $O_{\text{quantum total}} \approx O(1130 + 1) = O(1131)$.

Speedup: We can assess the comparative speedup advantage of the quantum approach versus the classical approach by computing the ratios of their respective complexities. The classical approach needs $O(7 \times 10^6)$, while the quantum approach requires $O(1131)$. This then translates to a speedup factor of approximately

$$\frac{7 \times 10^6}{1131} \approx 6188.$$

This means that the quantum approach is over 6000 times more computationally efficient than the classical approach for this problem.

By ‘faster’, we specifically mean that a quantum approach, as devised here, requires significantly fewer computational steps to arrive at the result. This reduction translates into less computational time, assuming similar hardware clock speeds and negligible algorithmic overhead and assuming a physical quantum computer with sufficiently stable logical qubits capable of encoding a circuit that encodes the construction we outline in this work.

In general, as the size of the network, $N = |V|$, increases, the computational advantage provided by the quantum approach becomes increasingly significant.

We can approximate a comparative scaling that shows how the speedup magnifies as N increases:

$$\sim \frac{O(N \cdot n)}{O(|S_n| \cdot 2^{n/2} + 1)}.$$

For large N , the classical complexity $O(N \cdot n)$ grows linearly, while the quantum complexity remains tied primarily to $|S_n|$ and $2^{n/2}$. This growing gap results in an increasingly significant computational advantage for the quantum approach.

For large-scale networks typical in the brain or artificial neural networks, N can be many billions of vertices. The classical approach will eventually become computationally infeasible due to its linear dependence on N , while the quantum approach remains algorithmically efficient. This scalability emphasizes the potential of a quantum approach like the one we developed here for analyzing the dynamics of large, high-dimensional networks.

7 Discussion

In this work, we introduced a novel class of problems related to the dynamics of large-scale networks relevant to neuroscience and machine learning. The problem we addressed asks whether a network can sustain inherent dynamic activity, cease functioning through quiescence, or saturate in an epileptic-like state. By carefully structuring the problem, we were able to take advantage of the unique properties of quantum computing, particularly the Deutsch–Jozsa and Grover algorithms, and provide an approach that solves this problem with significant computational efficiency compared to classical methods.

Classically, evaluating the dynamics of large networks requires an exhaustive search through the network’s state space, a computationally prohibitive task for very large networks. In contrast, the quantum approach we introduce here exploits superposition to evaluate the global state of the network in parallel, reducing the computational complexity by orders of magnitude.

The importance of this work lies in both its theoretical and practical implications. For neuroscience, it provides a potential novel tool to better model and understand the temporal and structural properties of neural networks. More broadly, it has potential applications in analyzing how brain dynamics relate to disorders associated with network disconnections, such as epilepsy, neurodevelopmental disorders such as Autism

Spectrum Disorder, and neural cognitive and degenerative disorders. In the context of machine learning and artificial intelligence, it is relevant to constructing and optimizing artificial neural network models. For quantum computing, this work serves as a proof-of-concept for how existing quantum algorithms can be adapted and extended to solve new, non-trivial interdisciplinary problems, motivating the continued exploration and expansion of quantum algorithms and computing.

7.1 Modeling the Evolution of Network Dynamics Beyond T_o

The framework and approach we introduce in this paper necessitate time evolving the network dynamics until the observation time T_o . A natural criticism is that if the dynamics can be evolved classically to reach T_o , it may be computationally simpler to continue evolving the system classically beyond T_o rather than leveraging a quantum approach. While this is a reasonable point, our intent here, in part, was to show that certain classes of problems related to network dynamics can be formally structured to give a quantum approach solution a computational advantage. In effect, it is a proof of concept example intended to motivate future work.

However, this consideration raises two broad areas in which quantum computing may contribute to the scientific study of neural networks. The first is large-scale simulations of neural dynamics across scales of spatial and temporal organization, bounded and informed by the known physiology (in the case of the brain) and known models (for artificial intelligence and machine learning). This is beyond the intent or scope of this paper. The second is carefully chosen and structured problems *about* neural dynamics that use quantum algorithms carefully and in a clever way, which we addressed in the current work. We propose they are necessarily complimentary rather than mutually exclusive or distinct.

Sufficiently large-scale simulations would allow observing, experimenting, and iterating numerical experiments under a wide range of parameter and model conditions. This is important because if, as neuroscientists suspect, complex emergent cognitive properties are partly due to sufficiently large interactions among foundational physiological and biological components and processes across temporal and spatial scales of organization, the need to carry out large iterative simulations may be critical to understanding or even just observing the dynamics that give rise to emergent cognitive properties. Simulations of this kind would support understanding emergent effects that depend on the scale of the computational space.

But open-ended large-scale simulations alone will not be sufficient for understanding how the brain, or artificial intelligence for that matter, works. In effect, open-ended large-scale simulations in isolation led to the significant challenges and missed targets faced by the highly publicized and hugely funded Blue Brain Project [14]. Arriving at a deep understanding necessitates carefully chosen and defined problems *about* the neural network dynamics being simulated. This is critical. Observing neural dynamics in action — for example, the firing patterns of large numbers of neurons — in isolation and without context alone cannot reveal the underlying algorithms operating on those dynamics or why they exist. It is no different than attempting to understand the brain from a systems perspective by studying a single participating protein or ion channel in isolation. Quantum computing potentially has a unique role in deciphering and understanding the contributions of functional network dynamics and behaviors on carefully formulated and constructed *interpretable* questions and problems, similar to what we do in this paper.

There may also be scenarios where, instead of a network model being simulated, a network evolves naturally according to its physical makeup, i.e., activity in the brain or internal activation patterns in artificial neural networks. In this scenario, only then are the dynamics measured or observed at some arbitrary time T_o to probe its behavior. In this case, as we showed here, a quantum computational approach to a well-structured question about the dynamics could be the only way to answer the question. This could have very real-world implications. The dynamics of the network may be inaccessible or uninterpretable before

or beyond T_o . For example, in biological neural networks, experimental limitations, such as noise, finite measurement windows, or ethical considerations, may constrain observations to specific time windows.

Our quantum framework and approach focus on evaluating the global state of the network at T_o all at once to infer its dynamic state and potential. Unlike classical methods, which necessitate the individual evaluation of each node and which quickly becomes computationally intractable, the quantum approach leverages superposition to assess the entire network state simultaneously. This enables insights into the network’s ability to sustain activity or transition between states without granular interrogation of the individual nodes that make up the network. The kind of framework we developed here provides a novel quantum computational lens for studying network dynamics.

7.2 Open Questions and Future Directions

While our work establishes a foundational framework, it also raises several important questions and opportunities for future research. First and foremost, while we showed a novel application of quantum computing to neural network dynamics and demonstrated significant computational speedup theoretically, implementing the approach we developed on current quantum hardware presents many practical challenges. Noise, decoherence, and the limited number of logical qubits in today’s quantum processors remain prohibitive limitations to modeling or computing properties of networks of any meaningful size. Future work could focus on testing our approach on new hardware and even adopt this as a benchmark problem.

We used the Deutsch–Jozsa and Grover algorithms in this work intentionally in part because we wanted to see if we could structure and solve a meaningful neural network problem by leveraging two foundational and extensively studied quantum algorithms. However, other quantum algorithms may offer complementary or even enhanced capabilities for similar types of problems. For example, algorithms designed for graph analysis or hybrid quantum-classical approaches could further expand the scope of network dynamics problems solvable by quantum computing.

In this paper and almost all of our prior published work on the neural dynamic model, we focused on fractional summation but deterministic network dynamics. However, in particular, neurons and neurobiological networks are inherently noisy and probabilistic. Extending the framework to account for stochastic dynamics is likely to be an important algorithmic strategy used by nature, but it raises new challenges about how to compute probabilistic states on quantum devices.

Lastly, in an even broader context, the methods developed here could inspire the design and engineering of quantum neural networks relevant to quantum machine learning that incorporate dynamic feedback mechanisms similar to biological neurons. Such networks could have applications in learning systems where temporal patterns and adaptive dynamics are critical.

Acknowledgments

The author would like to thank Robert Treuhaft, with whom he had some of the earliest conversations related to quantum computing and the brain. And to Eric Traut and Rita J. King for many insightful discussions and feedback.

References

- [1] Shor, P. W. Polynomial-time algorithms for prime factorization and discrete logarithms on a quantum computer. *SIAM Journal of Computation* **26**, 1484–1509 (1997).

- [2] Feynman, R. P. Simulating physics with computers. *International Journal of Theoretical Physics* **21**, 467–488 (1982).
- [3] Aspuru-Guzik, A., Dutoi, A. D., Love, P. J. & Head-Gordon, M. Simulated quantum computation of molecular energies. *Science* **309**, 1704–1707 (2005).
- [4] Preskill, J. Quantum computing in the nisq era and beyond. *arXiv* <https://arxiv.org/abs/1801.00862> (2018).
- [5] Fedorov, A. K., Gisin, N., Belousov, S. M. & Lvovsky, A. I. Quantum computing at the quantum advantage threshold: A down-to-business review *arXiv:2203.17181* (2022).
- [6] Au-Yeung, R., Camino, B., Rathore, O. & Kendon, V. Quantum algorithms for scientific applications *arXiv:2312.14904* (2023).
- [7] Buibas, M. & Silva, G. A. A framework for simulating and estimating the state and functional topology of complex dynamic geometric networks. *Neural Computation* **23**, 183–214 (2010).
- [8] Silva, G. A. The effect of signaling latencies and node refractory states on the dynamics of networks. *Neural Computation* **31**, 2492–2522 (2019).
- [9] Ezhikevich, E. M. Simple model of spiking neurons. *IEE Transactions on Neural Networks* **14**, 1569–1572 (2003).
- [10] Puppo, F., George, V. K. & Silva, G. A. An optimized function-structure design principle underlies efficient signaling dynamics in neurons. *Nature Scientific Reports* **8**, 10460 (2018).
- [11] George, V. K., Puppo, F. & Silva, G. A. Computing temporal sequences associated with dynamic patterns on the *C. elegans* connectome. *Frontiers in systems neuroscience* doi: 10.3389/fnsys.2021.564124 (2021).
- [12] George, V. K. *et al.* Learning without gradient descent encoded by the dynamics of a neurobiological network. *International Conference on Machine Learning (ICLR) Brain2AI* <https://arxiv.org/abs/2103.08878> (2021).
- [13] George, V. K., Morar, V. & Silva, G. A. A computational model for storing memories in the synaptic structures of the brain. *BioRxiv* <https://www.biorxiv.org/content/10.1101/2022.10.21.513291v1> (2023).
- [14] Documentary follows implosion of billion-euro brain project. *Nature* <https://www.nature.com/articles/d41586-020-03462-3>.